iScience

CellPress
OPEN ACCESS

Article

Immunosuppression-induced Zika virus reactivation causes brain inflammation and behavioral deficits in mice

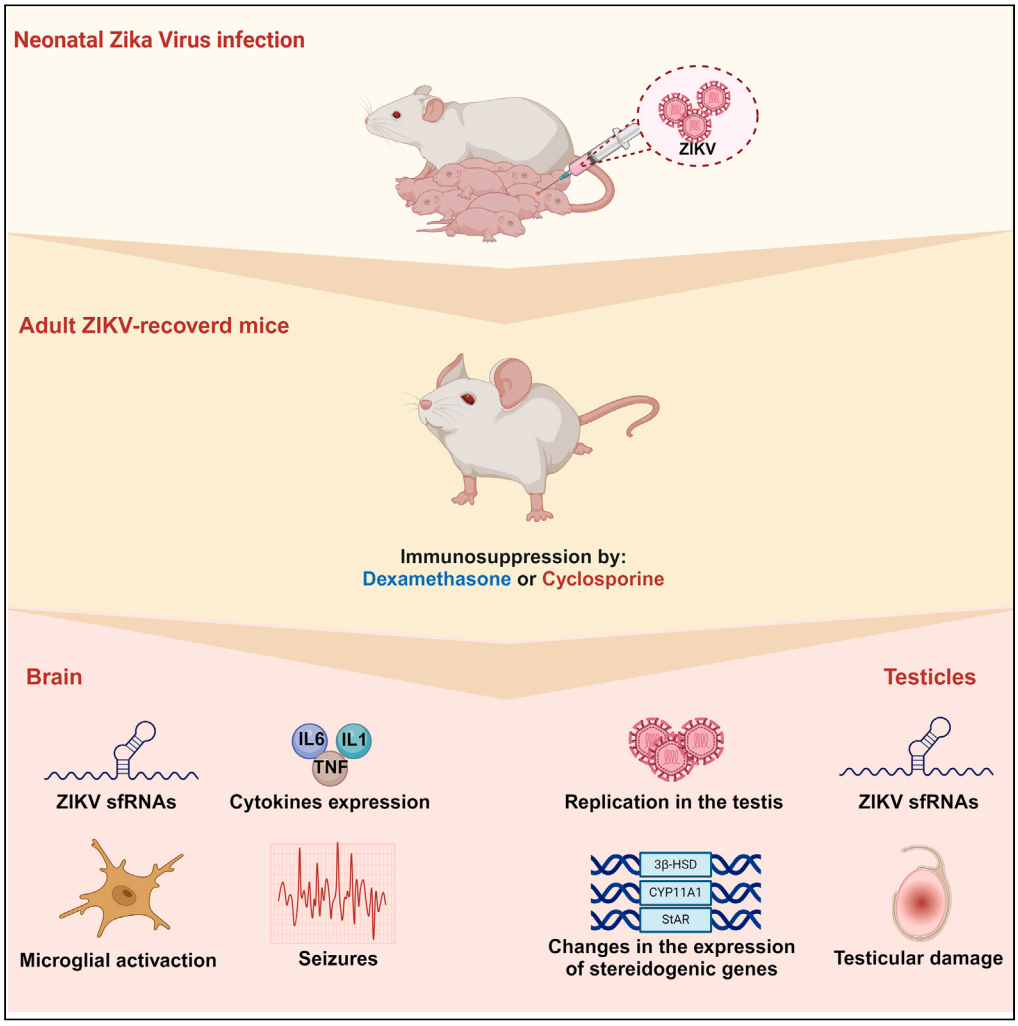

Clara de O. Nogueira, Mariana Oliveira Lopes da Silva, Emanuelle V. de Lima, ..., Iranaia Assunção-Miranda, Claudia P. Figueiredo, Julia R. Clarke

claufig@gmail.com (C.P.F.)
julia.clarke@icb.ufrj.br (J.R.C.)

Highlights

Immunosuppression late after ZIKV infection increases seizures in mice

Immunosuppression leads to viral replication late after ZIKV infection

Immunosuppression increases ZIKV sfRNA levels late after ZIKV infection

Immunosuppression leads to testicular damage late after ZIKV infection

Nogueira et al., iScience 27, 110178
July 19, 2024
https://doi.org/10.1016/j.isci.2024.110178

iScience

CellPress
OPEN ACCESS

Article

Immunosuppression-induced Zika virus reactivation causes brain inflammation and behavioral deficits in mice

Clara de O. Nogueira,[1] Mariana Oliveira Lopes da Silva,[2] Emanuelle V. de Lima,[1,3] Raíssa Rilo Christoff,[3] Daniel Gavino-Leopoldino,[2] Felipe S. Lemos,[3] Nicolas E. da Silva,[1] Andrea T. Da Poian,[4] Iranaia Assunção-Miranda,[2] Claudia P. Figueiredo,[1,3,*] and Julia R. Clarke[1,3,5,*]

SUMMARY

Zika virus (ZIKV) is a neurotropic flavivirus that can persist in several tissues. The late consequences of ZIKV persistence and whether new rounds of active replication can occur, remain unaddressed. Here, we investigated whether neonatally ZIKV-infected mice are susceptible to viral reactivation in adulthood. We found that when ZIKV-infected mice are treated with immunosuppressant drugs, they present increased susceptibility to chemically induced seizures. Levels of subgenomic flavivirus RNAs (sfRNAs) were increased, relative to the amounts of genomic RNAs, in the brains of mice following immunosuppression and were associated with changes in cytokine expression. We investigated the impact of immunosuppression on the testicles and found that ZIKV genomic RNA levels are increased in mice following immunosuppression, which also caused significant testicular damage. These findings suggest that ZIKV can establish new rounds of active replication long after acute stages of disease, so exposed patients should be monitored to ensure complete viral eradication.

INTRODUCTION

Zika virus (ZIKV) is a neurotropic flavivirus mainly transmitted by Aedes mosquitos, although transmission by vertical and sexual routes as well as by blood transfusions has already been reported.[1–3] Even though in most cases ZIKV infection causes a self-limited disease associated to mild symptoms, a myriad of neurologic complications has been reported in both adult subjects and, especially, in newborn babies following intrauterine exposure.[4,5] In addition, follow-up studies of the population exposed to ZIKV during the 2015 epidemics in the Americas suggest that even babies born without detectable brain alterations may show neurological symptoms due to viral exposure during critical stages of development.[6–8] Importantly, neurological symptoms have been reported long after flavivirus infection, even in patients that reported no sign of neurological damage during acute phases of infection.[9–11]

The acute and symptomatic phase of ZIKV disease lasts around ten days in humans, a stage during which infectious particles and viral genetic material can be detected in the blood. While in these patients viremia rapidly returns to undetectable levels after the acute phase of infection,[12,13] compelling evidence suggest that ZIKV can persist for long periods in several tissues and body fluids. Early studies performed in rodents and non-human primates have shown the ability of ZIKV to replicate and persist in several different tissues, such as the brain, lymph nodes, and testicles.[14–18] ZIKV RNA was detected in the placenta of pregnant women 200 days after infection[19] and on average 160 days in the brains of children born with congenital Zika syndrome (CZS).[20] Importantly, the male reproductive tract was shown to be an important site of viral persistence, and ZIKV was found in semen samples of infected men up to 93 days after the onset of symptoms.[21,22] The late consequences of ZIKV persistence remain poorly explored, and it remains unknown whether any environmental and physiological factors can potentially affect viral reactivation or the complete resolution of infection.

Some human pathogens, such as Herpes simplex and Varicella zoster, can establish latent infections, where new rounds of viral amplification, also called reactivation, may occur.[23,24] Although the exact mechanisms that lead to viral reactivation remain unknown, stress, nerve trauma, and immunosuppressant drugs were shown to contribute to trigger this phenomenon.[25] Some studies using murine models have suggested that encephalitic flaviviruses, such as West Nile virus (WNV), Japanese encephalitis virus (JEV), and tick-borne encephalitis virus (TBEV), can establish latent infections.[26–29] New rounds of active viral replication were shown when mice exposed *in utero* to JEV were treated with an immunosuppressant drug.[29,30] Likewise, WNV reactivation was observed in the brains of mice after twelve days of

[1]Faculdade de Farmácia, Universidade Federal do Rio de Janeiro, Rio de Janeiro 21941902, RJ, Brazil
[2]Instituto de Microbiologia Paulo de Goes, Universidade Federal do Rio de Janeiro, Rio de Janeiro 21941902, RJ, Brazil
[3]Instituto de Ciências Biomédicas, Universidade Federal do Rio de Janeiro, Rio de Janeiro 21941902, RJ, Brazil
[4]Instituto de Bioquímica Médica Leopoldo de Meis, Universidade Federal do Rio de Janeiro, Rio de Janeiro 21941902, RJ, Brazil
[5]Lead contact
*Correspondence: claufig@gmail.com (C.P.F.), julia.clarke@icb.ufrj.br (J.R.C.)
https://doi.org/10.1016/j.isci.2024.110178

cyclophosphamide-induced immunosuppression.[31] Despite the extensive evidence that ZIKV can persist in different tissues and body fluids, whether new rounds of active viral replication can occur has not yet been addressed.

Subgenomic flaviviral RNAs (sfRNAs) have been identified as critical regulators involved in viral replication and modulation of the hosts' immune response.[32–34] These genetic materials are products of incomplete degradation of viral genomic RNA by cellular exoribonucleases, resulting in accumulation of the conserved, highly structured, nuclease resistant, non-coding elements in the 3′ untranslated region (UTR). ZIKV sfRNAs are important for transplacental virus dissemination in pregnant mice and subsequent fetal brain infection.[35] Also, in human brain organoids ZIKV sfRNAs inhibit several antiviral pathways and promote apoptosis of neural progenitor cells[35] suggesting they have multiple biological roles in ZIKV pathogenesis. Still, little is known about the roles of sfRNAs late after ZIKV infection and whether they may contribute to viral persistence.

We previously demonstrated that neonatal ZIKV infection induces acute and chronic behavioral dysfunctions in mice, associated with viral RNA persistence in the brain for at least 100 days.[36] Here, we investigated whether immunosuppression can cause new rounds of viral amplification in mice late after ZIKV infection, and if this leads to increased susceptibility to seizures. ZIKV-infected mice treated with immunosuppressant drugs showed increased susceptibility to chemically induced seizures. While ZIKV genomic RNA levels remained constant in the brain following immunosuppression, we found increased brain generation of sfRNAs and changes in cytokine expression. We also investigated whether other important sites of viral persistence were affected. Since the testicles are an important site of viral replication and persistence,[17,37] we investigated the impact of immunosuppression on testicular morphology and function. We found that ZIKV genomic RNA levels increased in the testicles of mice following immunosuppression, which also caused significant testicular damage. These findings suggest that ZIKV establishes latent forms of infection and are susceptible to viral reactivation, which could impact the neurological outcome.

RESULTS

Dexamethasone-induced immunosuppression in ZIKV-infected mice increases susceptibility to seizures, with no increase in viral genomic RNA levels in the brain

Some viruses can establish persistent infections and undergo new rounds of active viral replication when the host is immunosuppressed. Here, Swiss mice at postnatal day 3 (P3) were infected with 10^6 PFU of ZIKV and treated with dexamethasone (DX) to induce immunosuppression when they reached adulthood (P60) (Figure 1A). As expected, DX treatment led to a significant decrease in the percentage of lymphocytes in peripheral blood in both control (mock-injected mice) and ZIKV-infected mice (Figure 1B), when compared to saline-treated groups (+Sal). Since weight loss is a hallmark of ongoing diseases in mice, we examined body weight of mice throughout DX treatment. Immunosuppression caused a significant decrease in body weight of ZIKV-infected mice at specific time points of DX treatment (Figure 1C; days 6, 8, and 9 of DX treatment), whereas the area under the curve (AUC) of body weight variations across treatment was significantly smaller for ZIKV+DX mice compared to saline-treated (Sal) groups (Figure 1D). We then investigated whether DX-induced immunosuppression caused locomotor impairment and increased susceptibility to chemically induced seizures in mice, as seen during acute stages of infection. No changes in locomotor activity were detected in ZIKV-infected animals (Figure 1E), regardless of treatment with DX or saline, as analyzed in the open field test. To assess whether immunosuppression would increase susceptibility of mice to seizures, animals were treated with the GABA antagonist pentylenetetrazol (PTZ). ZIKV-infected mice treated with saline or DX showed comparable time for first seizure following PTZ administration (Figure 1G). However, DX-immunosuppressed mice showed a significantly increased number of seizures when compared to all other groups (Figure 1G). To investigate whether behavioral changes in immunosuppressed mice were due to increased viral replication in the brain, levels of viral RNA and of ZIKV negative RNA strand, the template strand used for production of new copies of viral genetic material, were measured by qPCR. In agreement with our previous study,[36] both ZIKV positive and negative RNA strands were detected in the brains of untreated mice late (60 dpi) after infection, indicating RNA persistence (Figures 1H and 1I, black dots). However, no significant changes in brain viral RNAs were found following treatment with DX for 2, 5, or 10 days when compared to untreated mice (Figures 1H and 1I, blue dots). This finding was further confirmed in animals treated with an alternative immunosuppressant drug, cyclosporine (Cyclo, 30 mg/kg i.p.), a calcineurin inhibitor. As seen in DX-treated mice, ZIKV RNA levels were similar between groups of mice treated with Sal or Cyclo (Figure S1A).

Dexamethasone-induced immunosuppression in ZIKV-infected mice leads to increased generation of subgenomic flavivirus RNAs and altered expression of inflammatory mediators in the brain

sfRNAs are produced by incomplete degradation of flavivirus genomic RNA by cellular exoribonucleases. Mounting evidence suggests they have multiple roles in ZIKV pathogenesis, being especially important to determine viral persistence.[35] We next investigated whether sfRNAs could be detected in brains of mice after ZIKV infection, and whether immunosuppression had any effect on the levels of these noncoding genetic materials. Indeed, we found a significant increase in the detected levels of ZIKV noncoding RNAs in the brains of mice treated with DX (Figure 2A) or Cyclo (Figure 2B) for 10 days. We found a trend in increase on brain levels of mRNA coding exoribonuclease 1 (XRN-1), the main enzyme responsible for sfRNA generation inside host's cells, in infected mice following DX treatment (Figure 2C). XRN-1 expression was significantly upregulated in brains of mice following Cyclo treatment when compared to Sal-treated animals (Figure 2D). Microglial cells, the main brain-resident immune cells, are part of the first line of defense against ZIKV neuroinvasion, undergoing intense activation during acute stages of infection.[36,38–40] Non-coding RNAs were shown to modulate the expression of various pro-inflammatory cytokines and influence the degree of microglial activation in neurological diseases.[41–43] To investigate whether immunosuppression and sfRNA generation could enhance microglia/macrophage activation, we performed immunolabeling for the ionized calcium binding adaptor molecule 1 (Iba-1, a macrophage/microglial marker) in brain sections obtained from adult mice. While no changes in the number of macrophage/microglial cells were found

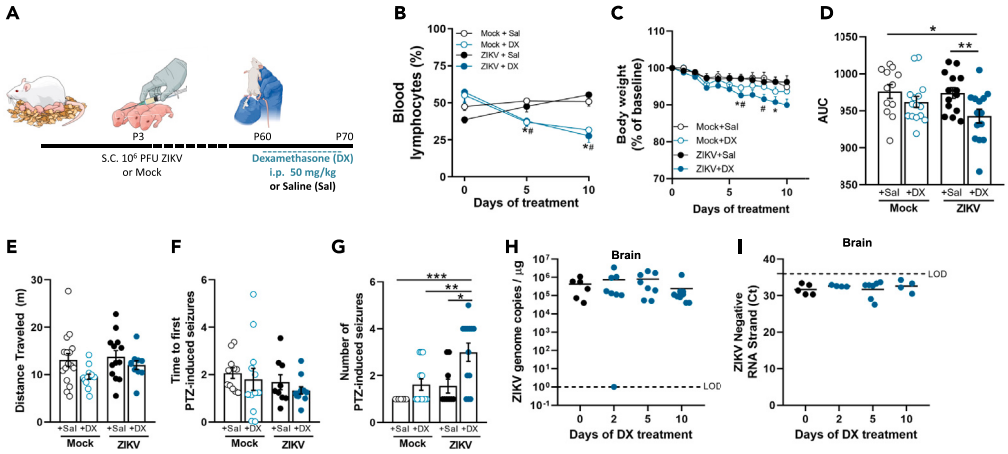

Figure 1. Dexamethasone-induced immunosuppression in ZIKV-infected mice increases susceptibility to seizures, with no increase in viral genomic RNA levels in the brain

(A) Mice at postnatal day 3 were infected with 10^6 PFU of ZIKV s.c. or received equal volume of mock medium. When animals reached adulthood, they were daily treated with dexamethasone (DX) or saline (Sal) i.p., for up to ten days.

(B) Percentage of lymphocytes in peripheral blood of ZIKV-infected and mock-injected mice before, or after 5 or 10 days of DX treatment. two-way ANOVA followed by Dunnet's post-hoc resulted in: *p = 0.0152 Mock+DX vs. Mock+Sal and #p = 0.0232 ZIKV+DX vs. Mock+Sal at 5 days of treatment. At 10 days of treatment: *p = 0.0009 Mock+DX vs. Mock+Sal and #p < 0.0001 ZIKV+DX vs. Mock+Sal. (n = 6 animals/group).

(C) Daily assessment of body weight of ZIKV-infected and mock-injected mice treated with Sal or DX (n = 12 Mock+Sal, 15 Mock+DX, 14 ZIKV+Sal, 14 ZIKV+DX). two-way ANOVA followed by Tukey post-hoc, *p = 0.0386 and 0.0397 ZIKV+DX vs. Mock+Sal. #p = 0.0062 and 0.0361 ZIKV+DX vs. ZIKV+Sal.

(D) Area under the curve (AUC) for body weight measured across treatment of ZIKV-infected and mock-injected mice treated with Sal or DX (n = 12 Mock+Sal, 15 Mock+DX, 14 ZIKV+Sal, 14 ZIKV+DX). Each symbol represents a different experimental subject. One-way ANOVA followed by Tukey post-hoc. *p = 0.0399 and **p = 0.0473.

(E) Distance traveled in the open field test by ZIKV-infected or mock-injected mice treated with saline (Sal) or dexamethasone (DX) for 10 days. One-way ANOVA followed by Tukey post-hoc revealed no difference between groups. N = 16 Mock+Sal, 14 Mock+DX, 13 ZIKV+Sal, 10 ZIKV+DX. Each symbol represents a different experimental subject.

(F) Time to first pentylenetetrazol-induced seizure shown by ZIKV-infected or mock-injected mice treated with Sal or DX for 10 days. N = 11 Mock+Sal, 12 Mock+DX, 9 ZIKV+Sal, 12 ZIKV+DX. One-way ANOVA followed by Tukey post-hoc revealed no difference between groups. Each symbol represents a different experimental subject.

(G) Number of pentylenetetrazol-induced seizures shown by ZIKV-infected or mock-injected mice treated with Sal or DX for 10 days. One-way ANOVA followed by Tukey post-hoc, *p = 0.0069, **p = 0.0039, ***p < 0.0001. N = 11 Mock+Sal, 13 Mock+DX, 9 ZIKV+Sal, 13 ZIKV+DX. Each symbol represents a different experimental subject.

(H and I) ZIKV genome copies (H; n = 6, 8, 8, and 9 for 0, 2, 5, and 10 days of treatment, respectively) and ZIKV negative RNA strand (I; n = 5, 4, 7, and 4 for 0, 2, 5, and 10 days of treatment, respectively) measured in the brains of mice before, or after 2, 5, or 10 days of DX treatment. One-way ANOVA followed by Tukey post-hoc revealed no difference between groups. Each symbol represents a different experimental subject. Data are expressed as means ± SEM.

between groups, Sholl analysis revealed that ZIKV infection led to a significantly decreased number of intersections of microglial cells when compared to mock-injected mice (Figures 2E–2G and 2I) indicative of the predominance of ameboid microglia in infected animals. However, immunosuppression was not associated to additional morphological changes in microglial cell morphology (Figures 2H and 2I). In addition, sfRNAs were shown to interfere with the host immune response,[33,44] decreasing IFN signaling to facilitate viral expansion. As could be expected, IFNβ mRNA levels were significantly increased in the brains of ZIKV-infected mice when compared to mock-injected mice. In contrast, immunosuppressed animals showed a significant reduction in IFNβ expression when compared to untreated animals (Figure 2J). No changes in the expression of the IFN downstream molecules ISG15 and OAS1 were observed after 10 days of DX treatment (Figures 2K and 2L). In addition, a significant increase in IL-1β expression (Figure 2M) and a trend of increase in IL-6 mRNA (Figure 2N) were found in the brains of ZIKV-infected immunosuppressed mice when compared with saline-treated or mock-injected animals. Similar levels of mRNA for TNF-α were found in the brains of ZIKV or mock injected mice, regardless of treatment (Figure 2O). These findings suggest that immunosuppression in ZIKV-infected mice results in increased brain levels of noncoding viral RNA and modulation of the neuroinflammatory response.

Dexamethasone-induced immunosuppression in ZIKV-infected mice causes testicular viral replication, morphological changes, and altered expression of steroidogenic pathway enzymes

Previous studies have shown that peripheral tissues are important sites of ZIKV amplification and persistence.[40,45–47] We hypothesized that new rounds of viral replication could occur in peripheral tissues under immunosuppressant conditions. We found that even though ZIKV RNA persisted in spleen and muscle, DX treatment was not sufficient to induce significant increase in viral genetic material (Figures 3A

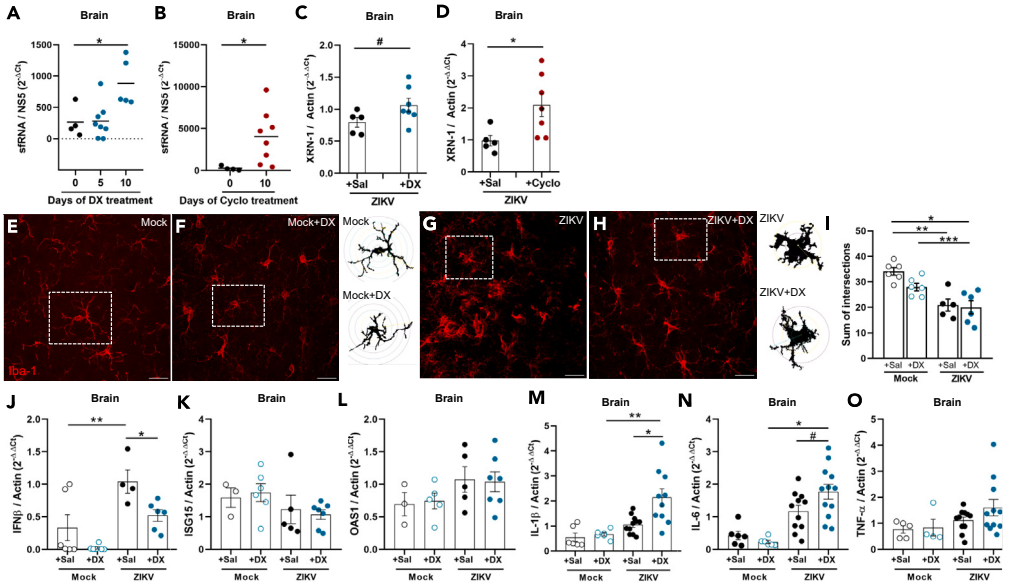

Figure 2. Dexamethasone-induced immunosuppression in ZIKV-infected mice leads to increased generation of subgenomic flavivirus RNAs and altered expression of inflammatory mediators in the brain

(A) Levels of ZIKV subgenomic flavivirus RNAs (sfRNAs) measured in the brains of infected mice before, or after 5 or 10 days of dexamethasone (DX) treatment. One-way ANOVA followed by Dunnett, $*p = 0.0171$. $N = 4, 8, 5$, for 0, 5, and 10 days of treatment, respectively. Each symbol represents a different experimental subject.

(B) Levels of ZIKV subgenomic flavivirus RNA (sfRNA) measured in the brains of infected mice before or after 10 days of cyclosporine (Cyclo) treatment. Student's *t* test, $*p = 0.0408$. $N = 4$ and 8 for 0 and 10 days of treatment, respectively. Each symbol represents a different experimental subject.

(C and D) Levels of XRN-1 mRNA were measured in the brains of infected mice treated with Sal or DX (C; $n = 5$ and 7 for 0 and 10 days of treatment, respectively) and Sal or Cyclo for 10 days (D; $n = 5$ and 7 for 0 and 10 days of treatment, respectively). Student's *t* test, $\#p = 0.0900$ and $*p = 0.033,3$, respectively). Each symbol represents a different experimental subject.

(E–H) Representative images of Sholl analysis in the brain of mock-injected mice treated with Sal (E) or DX (F), and ZIKV-infected mice treated with Sal (G) or DX (H) for 10 days. Individual cells highlighted in dashed-line rectangles are shown in the right of each representative image.

(I) Bar graph represents the number of intersections quantified in 4–6 cells per mouse. One-way ANOVA followed by Tukey $*p = 0.0004$ ZIKV+DX vs. Mock+Sal; $**p = 0.0011$ ZIKV+Sal vs. Mock+Sal; $***p = 0.0451$ ZIKV+DX vs. Mock+DX. Each symbol represents a different experimental subject.

(J–O) Levels of IFNβ (J, $n = 6$ Mock+Sal, 6 Mock+DX, 4 ZIKV+Sal, 6 ZIKV+DX), ISG15 (K, $n = 3$ Mock+Sal, 6 Mock+DX, 5 ZIKV+Sal, 7 ZIKV+DX), OAS1 (L, $n = 3$ Mock+Sal, 5 Mock+DX, 5 ZIKV+Sal, 7 ZIKV+DX), IL-1β (M; $n = 6$ Mock+Sal, 6 Mock+DX,11 ZIKV+Sal, 10 ZIKV+DX), IL-6 (N, $n = 6$ Mock+Sal, 6 Mock+DX,11 ZIKV+Sal, 12 ZIKV+DX) and TNF-α (O, $n = 5$ Mock+Sal, 4 Mock+DX, 11 ZIKV+Sal, 11 ZIKV+DX) mRNAs measured in the brains of infected mice treated with Sal or DX for 10 days. Actin was used as endogenous housekeeping gene. One-way ANOVA followed by Tukey, $**p = 0.0138$, $*p = 0.0199$ in J, $**p = 0.0011$, $*p = 0.0047$ in (M), $*p < 0.0001$, $\#p = 0.0556$ in (N). Data are representative of 2–3 independent experiments with similar results. Data are expressed as means ± SEM.

and 3B). Mounting evidence suggest that the male reproductive tract is an important site of ZIKV replication and persistence.[16,17,48] Thus, we evaluated whether DX-induced immunosuppression in adult mice neonatally exposed to ZIKV could lead to viral replication in the testicles. First, we confirmed that in our model the testicles are a site of early amplification of viral RNA (Figure S2A), but not sufficient to induce an increased expression of the pro-inflammatory cytokines TNF-α and IL-1β in this immune privileged tissue (Figures S2B and S2C). Moreover, while ZIKV RNA was cleared from the testes at 60 dpi (Figure 3C, black dots; Figure S2A), a significant increase in viral RNA was found following DX-induced immunosuppression, especially after 10 days of treatment (Figure 3C, blue dots). Further confirming the impact of immunosuppression on ZIKV testicular load, a significant increase in viral RNA was found in the testicles of Cyclo-treated mice when compared to infected group treated with Sal (Figure S2D). The epididymides, adjacent to the testicles, were not targeted by ZIKV during immunosuppression (Figure S2B), reinforcing a central role of the testes in viral replication. We next decided to characterize testicular damage caused by viral replication associated to immunosuppression. DX caused a significant increase in the weight of testicles of ZIKV-infected mice when compared to non-immunosuppressed infected mice (Figure 3D). Control experiments showed that ten days of DX treatment had no effect on testicle weight in mock-injected mice (Figure S2E), suggesting that change in gland weight is associated to viral replication. Histopathological analysis performed in HE-stained testicle slices revealed that some tissue damage caused by viral replication at early stages of infection persist until adulthood. Compared to mock-injected mice ($n = 5$; Figures 3E and 3F), testicles of infected mice ($n = 5$) revealed disrupted epithelium (present in 4 out of 5; Figure 3G black arrow) and hypertrophic and pale Sertoli cells (present in 1 out of 5), with no evident infiltration of inflammatory cells. Besides prominent disruption in epithelial integrity (Figure 3H black arrow), testicles of infected mice treated with DX for 10 days ($n = 6$) also revealed the presence of cells with morphological similarities to macrophages/monocytes, presenting cytoplasmic

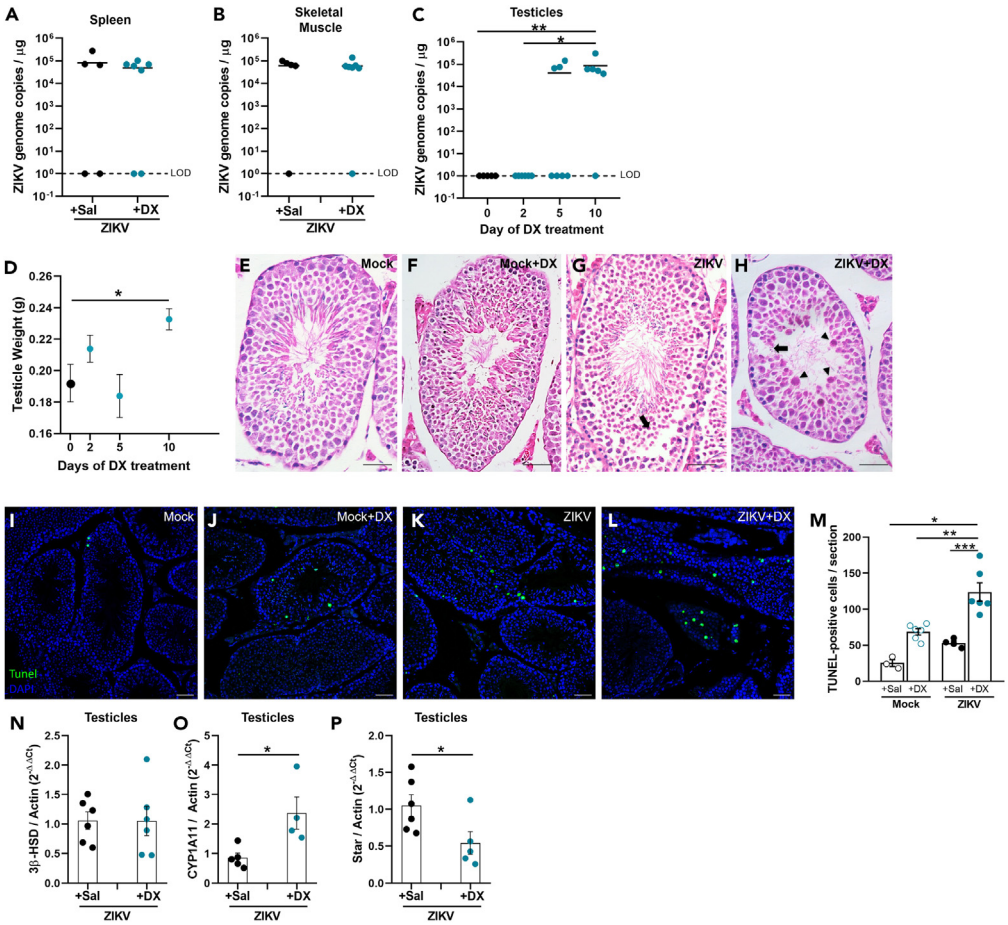

Figure 3. Dexamethasone-induced immunosuppression in ZIKV-infected mice causes testicular viral replication, morphological changes, and altered expression of steroidogenic pathway enzymes

(A and B) ZIKV genome copies measured in the spleen (A, $n = 5$ ZIKV+Sal, 7 ZIKV+DX) and skeletal muscle (B, $n = 5$ ZIKV+Sal, 7 ZIKV+DX) of infected mice treated with Sal or DX for 10 days. Each symbol represents a different experimental subject.

(C) ZIKV genome copies measured in the testicles of mice before, or after 2, 5 or 10 days of dexamethasone (DX) treatment. Mann-Whitney test, $*p = 0.0416$ and $*p = 0.0603$. $N = 5$, 6, 7 and 6 for 0, 2, 5 and 10 days of treatment, respectively. Each symbol represents a different experimental subject.

(D) Testicle weight of ZIKV-infected mice before or after 2, 5 or 10 days of DX treatment. One-way ANOVA followed by Tukey post-hoc, $*p = 0.0424$. $N = 9$, 10, 11, and 9 for 0, 2, 5, and 10 days of treatment, respectively. Each symbol represents a different experimental subject.

(E–H) Representative images of HE staining performed in testicles of mock-injected mice treated with Sal (E) or DX (F), or ZIKV-infected mice treated with Sal (G) or DX (H) for 10 days. Arrows indicate disrupted epithelium, and arrowheads indicate cells with cytoplasmic inclusions and macrophages/monocytes-similar cells. $N = 5$ Mock+Sal, 5 Mock+DX, 4 ZIKV+Sal, 6 ZIKV+DX. Scale bar, 50 µm.

(I–M) Representative images of TUNEL immunostaining in the testicles of mock-injected mice treated with Sal (I) or DX (J), or ZIKV-infected mice treated with Sal (K) or DX (L) for 10 days (M) Bar graph represents the number of TUNEL-positive cells. One-way ANOVA followed by Tukey $*p < 0.0001$ ZIKV+DX vs. Mock+Sal; $**p = 0.0009$ ZIKV+DX vs. Mock+DX; $***p = 0.0002$ ZIKV+DX vs. ZIKV+Sal. $N = 3$ Mock+Sal, 6 Mock+DX, 4 ZIKV+Sal, 6 ZIKV+DX. Each symbol represents a different experimental subject.

(N–P) Levels of 3β-HSD (N, $n = 6$/group), CYP11A1 (O, $n = 5$ ZIKV+Sal, 4 ZIKV+DX) and StAR (P, $n = 6$ ZIKV+Sal, 5 ZIKV+DX) mRNA detected in the testicles of ZIKV-infected mice treated with Sal or DX for 10 days. Student's t test, $*p = 0.0211$ in (O), $*p = 0.0423$ in (P). Each symbol represents a different experimental subject. Data are expressed as means ± SEM.

inclusions ($n = 2$ out of 6; Figure 3H black arrowheads). Presence of macrophage-like cells coincided with regions of increased epithelium damage. Events of karyomegaly and cytomegaly in apical regions of the seminal tubules were also found in one animal. TUNEL assay was performed in the testicles of mice, revealing a significantly increased number of apoptotic cells in ZIKV-infected mice treated with DX, when compared to Sal-treated groups (Figures 3I–3M). We next evaluated if DX treatment interfered with gene expression of enzymes involved in testosterone synthesis. While levels of 3β hydroxysteroid dehydrogenase (3β-HSD) mRNA were not altered by DX treatment in ZIKV infected mice (Figure 3N), expression of cytochrome P450 family 11 subfamily A1 (CYP11A1) and steroidogenic acute regulatory protein (StAR) were significantly increased (Figure 3O) and decreased (Figure 3P), respectively, in the testicles of infected mice upon

immunosuppression. Ruling out the possibility that this was an unspecific effect of DX treatment per se, DX- and Sal-treated mice that were not previously exposed to the virus showed comparable mRNA levels for these targets (Figures S2F–S2H). Since the female reproductive tract has also been suggested as an important site of ZIKV amplification,[15,49,50] we also performed viral RNA quantification in the ovaries of infected mice. ZIKV nucleic acid levels were below the limit of detection in all samples analyzed—at least 3 samples from each of the following groups: 0, 2, 5, and 10 days after DX treatment, as well as 10 days after Cyclo treatment. Altogether, our findings suggest that ZIKV can establish new rounds of viral RNA replication long after acute stages of disease in mice. These new rounds of replication and generation of sfRNAs may contribute to the observed behavioral alterations.

DISCUSSION

ZIKV infection during pregnancy causes serious neurological conditions, including microcephaly, in newborns. Mounting evidence suggest that the virus can persist in several different tissues and body fluids, both in newborn babies exposed *in utero* and in adult subjects.[14–16,18–20] Nonetheless, whether and which late consequences can derive from the presence of these long-lasting viral particles remain unclear. To address this gap, we here investigated whether new rounds of active ZIKV replication and behavioral/neurological deficits could be induced in mice. We have previously shown that ZIKV systemic infection in mice at postnatal day 3 results in brain replication, reaching a peak at 6 days post infection.[36] Here, animals that survived the acute phase of ZIKV infection were submitted to an immunosuppressant protocol with DX when they reached adulthood. Dexamethasone immunosuppression has been used to increase susceptibility of wild-type adult mice to ZIKV infection.[47] Using the same dose, we found that DX treatment in mice promoted significant changes in the leukocyte population in peripheral blood, suggestive of immunosuppression.[51]

Weight loss is an important hallmark of sickness behavior typical of ongoing infections in mouse models.[36,40,47] Here, even though immunosuppression was found in both mock-injected and ZIKV-infected mice, weight loss was only observed in virus-exposed mice. These findings ruled out an unspecific effect of corticosteroid treatment and suggested the occurrence of ongoing ZIKV amplification. In addition, systemic immunosuppression late after ZIKV infection led to increased number of seizures in mice suggesting that a decreased immune response interferes with behavioral outcome in situations where viral RNA persists in nervous tissue. The nervous system is a central site of ZIKV replication and persistence in animal models and humans.[14,19,20,52] The possibility that brain residual ZIKV could undergo new rounds of active replication has been raised,[53] but experimental evidences were lacking. Our results show that immunosuppression was not associated to net increase in viral genomic RNA in the mouse brain late after infection. However, accumulation of sfRNAs were found in the brains of DX- and Cyclo-treated mice, suggesting that immunosuppression caused an increase in degradation of viral RNA by cellular exoribonucleases, which we found to be upregulated. Importantly, sfRNAs have been given much attention recently, because they have been identified as critical regulators involved in flavivirus replication and pathogenesis.[32,33,54,55] These conserved, highly structured, nuclease resistant, non-coding elements in the 3′ untranslated region (UTR) were shown to interfere with different intracellular signaling pathways, including interferon-β-mediated,[55] to facilitate viral amplification.[33] In addition, ZIKV sfRNAs are important for transplacental virus dissemination in pregnant mice, fetal brain infection and can promote apoptosis of neural progenitor cells.[35] We further found that DX treatment did not interfere with morphology of microglia/macrophage cells when compared to ZIKV-infected mice which were not exposed to immunosuppressant treatment, suggesting that infection *per se* plays a more relevant role on microglial morphology than DX treatment, even at 60 d.p.i. Morphological changes in microglial cells are classically considered indicative of activation of these innate immune cells. However, it is known that activated microglial cells may change their secretory profile even in the absence of morphological changes.[56] In our study, the increased generation of ZIKV sfRNAs in the brains of immunosuppressed mice was accompanied by changes in expression of cytokines such as IFNβ, IL-1β, and IL6. Increased brain expression of these inflammatory mediators has been reported during acute stages of ZIKV infection[36,57] and correlated with behavioral changes in different animal models.[53,58,59] Our group has previously shown that increased cytokine production in the brains of mice is crucial for late behavioral impairment associated to ZIKV exposure during development. Moreover, inflammation blockage during critical time frames efficiently prevents the increased susceptibility to chemically induced seizures caused by infection.[36]

In several studies, ZIKV has been detected in the male reproductive tract during acute phases of infection, persisting in the testicular somatic, germ cells, and spermatozoa.[16,17,60,61] Maintenance of an immune-privileged environment in the testes is essential for healthy spermatogenesis, but this contributes for viral sheltering in this tissue. Viral persistence in these sites may be responsible for male-to-female and male-to-male sexual transmission several months after disease.[62] We found that under immunosuppression, the testicles are central sites of viral RNA replication late after ZIKV infection. It remains to be determined whether the synthesis of new copies of viral genome translates into the generation of infective viral particles, which would be especially concerning for reemergence of sexual transmission. We also found that other parts of the male reproductive tract, such as the epididymis, were not targeted by ZIKV during immunosuppression, reinforcing a central role of the testes in viral replication. Some studies reported that ZIKV can also persist in the female reproductive tract.[15,49,50] In contrast, we found that the ovaries were not a site of RNA persistence nor were new rounds of viral replication detected upon immunosuppression. Considering that viral RNA was not detectable in the testicles before DX treatment began, these results comprise original evidence that persistent ZIKV RNA invades new sites for replication under adverse conditions. The clinical impact of these findings, i.e., whether new rounds of sexual infectivity can occur in immunosuppressed patients, should be determined.

Changes in the expression of enzymes involved in testosterone synthesis have been reported during acute stages of ZIKV infection in mice,[37] resulting in altered testosterone levels.[17] The first and rate-limiting step is the transport of cholesterol into mitochondria which is mediated by the high-affinity cholesterol binding protein StAR. Cholesterol is then targeted by CYP11A1, which performs three sequential oxidation reactions originating pregnenolone. The amount of CYP11A1 protein determinates the biosynthetic capacity of testicle Leydig cells, and

is primarily decided by transcription of CYP11A gene. Importantly, expression of StAR and CYP11A were shown to be affected by aging,[63–65] inflammation,[66] oxidative stress[67,68] among others. In our study, we found that DX treatment of ZIKV-infected mice induced downregulation of StAR gene and upregulation of CYP11A1, when compared to infected mice treated with saline. Our hypothesis for the opposite effects of treatment on expression of these two genes, is that once the transport of cholesterol into the inner mitochondrial membrane is impaired by reduced levels of StAR, CYP11A1 gene is upregulated as an attempt to maintain testosterone synthesis in normal levels. However, in the context of our study, these show that immunosuppression of infected mice leads to disruption of normal testicular function like those seen during acute stages of ZIKV replication, or in situations of testicular inflammation and oxidative stress. Abnormal sperm count, motility, and morphology have already been reported in ZIKV-recovered patients, up to one year after clinical confirmation of infection.[69,70] These findings raise a concern about male fertility in ZIKV recovered patients, indicating that besides long-term neurological assessment, endocrine system and reproductive systems follow up may be required.

In conclusion, our results suggest that patients should be monitored to ensure the complete eradication of ZIKV following intrauterine or early-life exposure. Moreover, therapies targeting viral clearance should be pursued whereas immunosuppressant therapies in ZIKV-recovered patients should be performed with caution.

Limitations of the study

Although our study provides clear evidence that ZIKV can undergo new rounds of RNA replication, our study has a few limitations. First, we were unable to quantify whether replication of viral genome in conditions of immunosuppression leads to generation of infective particles. It is still uncertain whether methodological limitations are the cause of failure of plaque assays, or whether assembly of infective ZIKV particles is blocked by cells at these chronic stages of infection. In addition, the sfRNA species found to be increased in brains and testicles of mice should be further characterized in the future by techniques such as northern blot. Finally, our results cannot be extrapolated to conditions such as stress, in which immunosuppression usually occurs. Further studies should be performed to confirm our findings under such circumstances.

STAR★METHODS

Detailed methods are provided in the online version of this paper and include the following:

- KEY RESOURCES TABLE
- RESOURCE AVAILABILITY
  - Lead contact
  - Materials availability
  - Data and code availability
- EXPERIMENTAL MODEL AND STUDY PARTICIPANT DETAILS
  - Experimental design
  - Animals
- METHOD DETAILS
  - Virus
  - Viral infections
  - Pharmacological treatments
  - Behavioral tests
- QUANTIFICATION AND STATISTICAL ANALYSIS
  - Statistical analysis

SUPPLEMENTAL INFORMATION

Supplemental information can be found online at https://doi.org/10.1016/j.isci.2024.110178.

ACKNOWLEDGMENTS

We thank funding agencies *Fundação de Amparo à Pesquisa no Estado do Rio de Janeiro* (grant number 26/202.740/2019) and *Conselho Nacional de Desenvolvimento Científico e Tecnológico* (grant number 305511/2018-1).

AUTHOR CONTRIBUTIONS

C.O.N., E.V.L., and N.E.S. planned and performed infections and behavioral experiments in mice. M.O.L.S. and D.G. obtained viral stocks and performed viral RNA quantification. C.O.N. and M.O.L.S. performed gene expression experiments. R.R.C. and F.S.L. performed histological and immunohistochemistry analysis. A.T.P., I.A.M., C.P.F., and J.R.C. planned and supervised experiments, wrote manuscript and obtained funding sources.

DECLARATION OF INTERESTS

The authors declare no conflict of interest.

Received: November 27, 2023
Revised: February 27, 2024
Accepted: May 31, 2024
Published: June 5, 2024

REFERENCES

1. Foy, B.D., Kobylinski, K.C., Chilson Foy, J.L., Blitvich, B.J., Travassos da Rosa, A., Haddow, A.D., Lanciotti, R.S., and Tesh, R.B. (2011). Probable Non–Vector-borne Transmission of Zika Virus, Colorado, USA. Emerg. Infect. Dis. *17*, 880–882. https://doi.org/10.3201/eid1705.101939.
2. Hastings, A.K., and Fikrig, E. (2017). Zika Virus and Sexual Transmission: A New Route of Transmission for Mosquito-borne Flaviviruses. Yale J. Biol. Med. *90*, 325–330.
3. Jimenez, A., Shaz, B.H., and Bloch, E.M. (2017). Zika Virus and the Blood Supply: What Do We Know? Transfus. Med. Rev. *31*, 1–10. https://doi.org/10.1016/j.tmrv.2016.08.001.
4. Krauer, F., Riesen, M., Reveiz, L., Oladapo, O.T., Martínez-Vega, R., Porgo, T.V., Haefliger, A., Broutet, N.J., and Low, N.; WHO Zika Causality Working Group (2017). Zika Virus Infection as a Cause of Congenital Brain Abnormalities and Guillain–Barré Syndrome: Systematic Review. PLoS Med. *14*, e1002203. https://doi.org/10.1371/journal.pmed.1002203.
5. Rasmussen, S.A., Jamieson, D.J., Honein, M.A., and Petersen, L.R. (2016). Zika Virus and Birth Defects — Reviewing the Evidence for Causality. N. Engl. J. Med. *374*, 1981–1987. https://doi.org/10.1056/NEJMsr1604338.
6. Walker, C.L., Little, M.-T.E., Roby, J.A., Armistead, B., Gale, M., Rajagopal, L., Nelson, B.R., Ehinger, N., Mason, B., Nayeri, U., et al. (2019). Zika virus and the nonmicrocephalic fetus: why we should still worry. Am. J. Obstet. Gynecol. *220*, 45–56. https://doi.org/10.1016/j.ajog.2018.08.035.
7. Mulkey, S.B., Arroyave-Wessel, M., Peyton, C., Bulas, D.I., Fourzali, Y., Jiang, J., Russo, S., McCarter, R., Msall, M.E., du Plessis, A.J., et al. (2020). Neurodevelopmental Abnormalities in Children With In Utero Zika Virus Exposure Without Congenital Zika Syndrome. JAMA Pediatr. *174*, 269–276. https://doi.org/10.1001/jamapediatrics.2019.5204.
8. Van der Linden, V., Pessoa, A., Dobyns, W., Barkovich, A.J., Júnior, H.v.d.L., Filho, E.L.R., Ribeiro, E.M., Leal, M.d.C., Coimbra, P.P.d.A., Aragão, M.d.F.V.V., et al. (2016). Description of 13 Infants Born During October 2015-January 2016 With Congenital Zika Virus Infection Without Microcephaly at Birth - Brazil. MMWR Morb. Mortal Wkly. Rep. *65*, 1343–1348. https://doi.org/10.15585/mmwr.mm6547e2.
9. Chen, H.-Y., Yang, C.-Y., Hsieh, C.-Y., Yeh, C.-Y., Chen, C.-C., Chen, Y.-C., Lai, C.-C., Harris, R.C., Ou, H.-T., Ko, N.-Y., and Ko, W.C. (2021). Long-term neurological and healthcare burden of adults with Japanese encephalitis: A nationwide study 2000-2015. PLoS Neglected Trop. Dis. *15*, e0009703. https://doi.org/10.1371/journal.pntd.0009703.
10. Singhi, P. (2011). Infectious causes of seizures and epilepsy in the developing world. Dev. Med. Child Neurol. *53*, 600–609. https://doi.org/10.1111/j.1469-8749.2011.03928.x.
11. Edupuganti, S., Natrajan, M.S., Rouphael, N., Lai, L., Xu, Y., Feldhammer, M., Hill, C., Patel, S.M., Johnson, S.J., Bower, M., et al. (2017). Biphasic Zika Illness With Rash and Joint Pain. Open Forum Infect. Dis. *4*, ofx133. https://doi.org/10.1093/ofid/ofx133.
12. Barzon, L., Pacenti, M., Berto, A., Sinigaglia, A., Franchin, E., Lavezzo, E., Brugnaro, P., and Palù, G. (2016). Isolation of infectious Zika virus from saliva and prolonged viral RNA shedding in a traveller returning from the Dominican Republic to Italy, January 2016. Euro Surveill. *21*, 30159. https://doi.org/10.2807/1560-7917.ES.2016.21.10.30159.
13. Lanciotti, R.S., Kosoy, O.L., Laven, J.J., Velez, J.O., Lambert, A.J., Johnson, A.J., Stanfield, S.M., and Duffy, M.R. (2008). Genetic and Serologic Properties of Zika Virus Associated with an Epidemic , Yap State , Micronesia, 2007. Emerg. Infect. Dis. *14*, 1232–1239. https://doi.org/10.3201/eid1408.080287.
14. Aid, M., Abbink, P., Larocca, R.A., Boyd, M., Nityanandam, R., Nanayakkara, O., Martinot, A.J., Moseley, E.T., Blass, E., Borducchi, E.N., et al. (2017). Zika Virus Persistence in the Central Nervous System and Lymph Nodes of Rhesus Monkeys. Cell *169*, 610–620.e14. https://doi.org/10.1016/j.cell.2017.04.008.
15. Hirsch, A.J., Smith, J.L., Haese, N.N., Broeckel, R.M., Parkins, C.J., Kreklywich, C., DeFilippis, V.R., Denton, M., Smith, P.P., Messer, W.B., et al. (2017). Zika Virus infection of rhesus macaques leads to viral persistence in multiple tissues. PLoS Pathog. *13*, e1006219. https://doi.org/10.1371/journal.ppat.1006219.
16. Ball, E.E., Pesavento, P.A., Van Rompay, K.K.A., Keel, M.K., Singapuri, A., Gomez-Vazquez, J.P., Dudley, D.M., O'Connor, D.H., Breitbach, M.E., Maness, N.J., et al. (2022). Zika virus persistence in the male macaque reproductive tract. PLoS Neglected Trop. Dis. *16*, e0010566. https://doi.org/10.1371/journal.pntd.0010566.
17. Govero, J., Esakky, P., Scheaffer, S.M., Fernandez, E., Drury, A., Platt, D.J., Gorman, M.J., Richner, J.M., Caine, E.A., Salazar, V., et al. (2016). Zika virus infection damages the testes in mice. Nature *540*, 438–442. https://doi.org/10.1038/nature20556.
18. Hsu, D.C., Chumpolkulwong, K., Corley, M.J., Hunsawong, T., Inthawong, D., Schuetz, A., Imerbsin, R., Silsorn, D., Nadee, P., Sopanaporn, J., et al. (2022). Neurocognitive impact of Zika virus infection in adult rhesus macaques. J. Neuroinflammation *19*, 40. https://doi.org/10.1186/s12974-022-02402-4.
19. Bhatnagar, J., Rabeneck, D.B., Martines, R.B., Reagan-Steiner, S., Ermias, Y., Estetter, L.B.C., Suzuki, T., Ritter, J., Keating, M.K., Hale, G., et al. (2017). Zika Virus RNA Replication and Persistence in Brain and Placental Tissue. Emerg. Infect. Dis. *23*, 405–414. https://doi.org/10.3201/eid2303.161499.
20. Chimelli, L., Moura Pone, S., Avvad-Portari, E., Farias Meira Vasconcelos, Z., Araújo Zin, A., Prado Cunha, D., Raposo Thompson, N., Lopes Moreira, M.E., Wiley, C.A., and da Silva Pone, M.V. (2018). Persistence of Zika Virus After Birth: Clinical, Virological, Neuroimaging, and Neuropathological Documentation in a 5-Month Infant With Congenital Zika Syndrome. J. Neuropathol. Exp. Neurol. *77*, 193–198. https://doi.org/10.1093/jnen/nlx116.
21. Medina, F.A., Torres, G., Acevedo, J., Fonseca, S., Casiano, L., De León-Rodríguez, C.M., Santiago, G.A., Doyle, K., Sharp, T.M., Alvarado, L.I., et al. (2019). Duration of the Presence of Infectious Zika Virus in Semen and Serum. J. Infect. Dis. *219*, 31–40. https://doi.org/10.1093/infdis/jiy462.
22. Oliveira, I., Alejo-cancho, I., Gascón, J., Peiró, A., and Mu, J. (2018). Persistence of Zika virus in semen 93 days after the onset of symptoms Inés. Enferm. Infecc. Microbiol. Clín. *36*, 21–23. https://doi.org/10.1016/j.eimc.2016.10.009.
23. Grinde, B. (2013). Herpesviruses: latency and reactivation - viral strategies and host response. J. Oral Microbiol. *5*, 22766. https://doi.org/10.3402/jom.v5i0.22766.
24. Nagel, M.A., and Gilden, D. (2013). Complications of varicella zoster virus reactivation. Curr. Treat. Options Neurol. *15*, 439–453. https://doi.org/10.1007/s11940-013-0246-5.
25. Traylen, C.M., Patel, H.R., Fondaw, W., Mahatme, S., Williams, J.F., Walker, L.R., Dyson, O.F., Arce, S., and Akula, S.M. (2011). Virus reactivation: a panoramic view in human infections. Future Virol. *6*, 451–463. https://doi.org/10.2217/fvl.11.21.
26. Honig, A., and Karussis, D. (2014). Delayed-onset flaccid paralysis related to west Nile virus reactivation following treatment with rituximab: a case report. BMC Res. Notes *7*, 852. https://doi.org/10.1186/1756-0500-7-852.
27. Beardsley, R., and McCannel, C. (2012). Reactivation West Nile Virus Infection-related Chorioretinitis. Semin. Ophthalmol. *27*, 43–45. https://doi.org/10.3109/08820538.2011.631512.
28. Volok, V.P., Gmyl, L.V., Belyaletdinova, I.K., Karganova, G.G., and Dekonenko, E.P. (2022). Progressive Course of Chronic Tick-Borne Encephalitis Manifesting as Amyotrophic Lateral Sclerosis-like Syndrome 35 Years after the Acute Disease. Brain Sci. *12*, 1020. https://doi.org/10.3390/brainsci12081020.
29. Mathur, A., Kulshreshtha, R., and Chaturvedi, U.C. (1987). Induction of secondary immune response by reactivated Japanese encephalitis virus in latently infected mice. Immunology *60*, 481–484.
30. Mathur, A., Arora, K.L., Rawat, S., and Chaturvedi, U.C. (1986). Persistence, Latency and Reactivation of Japanese Encephalitis Virus Infection in Mice. J. Gen. Virol. *67*, 381–385. https://doi.org/10.1099/0022-1317-67-2-381.
31. Appler, K.K., Brown, A.N., Stewart, B.S., Behr, M.J., Demarest, V.L., Wong, S.J., and Bernard, K.A. (2010). Persistence of West Nile virus in the central nervous system and

periphery of mice. PLoS One *5*, e10649. https://doi.org/10.1371/journal.pone.0010649.
32. Manokaran, G., Finol, E., Wang, C., Gunaratne, J., Bahl, J., Ong, E.Z., Tan, H.C., Sessions, O.M., Ward, A.M., Gubler, D.J., et al. (2015). Dengue subgenomic RNA binds TRIM25 to inhibit interferon expression for epidemiological fitness. Science *350*, 217–221. https://doi.org/10.1126/science.aab3369.
33. Pijlman, G.P., Funk, A., Kondratieva, N., Leung, J., Torres, S., van der Aa, L., Liu, W.J., Palmenberg, A.C., Shi, P.-Y., Hall, R.A., and Khromykh, A.A. (2008). A highly structured, nuclease-resistant, noncoding RNA produced by flaviviruses is required for pathogenicity. Cell Host Microbe *4*, 579–591. https://doi.org/10.1016/j.chom.2008.10.007.
34. Slonchak, A., and Khromykh, A.A. (2018). Subgenomic flaviviral RNAs: What do we know after the first decade of research. Antivir. Res. *159*, 13–25. https://doi.org/10.1016/j.antiviral.2018.09.006.
35. Slonchak, A., Wang, X., Aguado, J., Sng, J.D.J., Chaggar, H., Freney, M.E., Yan, K., Torres, F.J., Amarilla, A.A., Balea, R., et al. (2022). Zika virus noncoding RNA cooperates with the viral protein NS5 to inhibit STAT1 phosphorylation and facilitate viral pathogenesis. Sci. Adv. *8*, eadd8095. https://doi.org/10.1126/sciadv.add8095.
36. Souza, I.N., Frost, P.S., França, J.V., Nascimento-Viana, J.B., Neris, R.L.S., Freitas, L., Pinheiro, D.J.L.L., Nogueira, C.O., Neves, G., Chimelli, L., et al. (2018). Acute and chronic neurological consequences of early-life zika virus infection in mice. Sci. Transl. Med. *10*, 1–11. https://doi.org/10.1126/scitranslmed.aar2749.
37. Uraki, R., Hwang, J., Jurado, K.A., Householder, S., Yockey, L.J., Hastings, A.K., Homer, R.J., Iwasaki, A., and Fikrig, E. (2017). Zika virus causes testicular atrophy. Sci. Adv. *3*, e1602899. https://doi.org/10.1126/sciadv.1602899.
38. Lum, F.-M., Low, D.K.S., Fan, Y., Tan, J.J.L., Lee, B., Chan, J.K.Y., Rénia, L., Ginhoux, F., and Ng, L.F.P. (2017). Zika Virus Infects Human Fetal Brain Microglia and Induces Inflammation. Clin. Infect. Dis. *64*, 914–920. https://doi.org/10.1093/cid/ciw878.
39. Lawrence, J.H., Sherer, M.L., Tavlarides-Hontz, P., Parcells, M.S., and Schwarz, J.M. (2019). An investigation into the immune response of cultured neural rat cells following Zika virus infection. J. Neuroimmunol. *332*, 73–77. https://doi.org/10.1016/j.jneuroim.2019.04.002.
40. Figueiredo, C.P., Barros-Aragão, F.G.Q., Neris, R.L.S., Frost, P.S., Soares, C., Souza, I.N.O., Zeidler, J.D., Zamberlan, D.C., de Sousa, V.L., Souza, A.S., et al. (2019). Zika virus replicates in adult human brain tissue and impairs synapses and memory in mice. Nat. Commun. *10*, 3890. https://doi.org/10.1038/s41467-019-11866-7.
41. Tripathi, S., Shree, B., Mohapatra, S., Sharma, V., Basu, A., and Basu, A. (2021). The Expanding Regulatory Mechanisms and Cellular Functions of Long Non-coding RNAs (lncRNAs) in Neuroinflammation. Mol. Neurobiol. *58*, 2916–2939. https://doi.org/10.1007/s12035-020-02268-8.
42. Shi, Z., Pan, B., and Feng, S. (2018). The emerging role of long non-coding RNA in spinal cord injury. J. Cell Mol. Med. *22*, 2055–2061. https://doi.org/10.1111/jcmm.13515.
43. Chen, M., Lai, X., Wang, X., Ying, J., Zhang, L., Zhou, B., Liu, X., Zhang, J., Wei, G., and Hua, F. (2021). Long Non-coding RNAs and Circular RNAs: Insights Into Microglia and Astrocyte Mediated Neurological Diseases. Front. Mol. Neurosci. *14*, 745066. https://doi.org/10.3389/fnmol.2021.745066.
44. Schuessler, A., Funk, A., Lazear, H.M., Cooper, D.A., Torres, S., Daffis, S., Jha, B.K., Kumagai, Y., Takeuchi, O., Hertzog, P., et al. (2012). West Nile Virus Noncoding Subgenomic RNA Contributes to Viral Evasion of the Type I Interferon-Mediated Antiviral Response. J. Virol. *86*, 5708–5718. https://doi.org/10.1128/JVI.00207-12.
45. Mustafá, Y.M., Meuren, L.M., Coelho, S.V.A., and de Arruda, L.B. (2019). Pathways Exploited by Flaviviruses to Counteract the Blood-Brain Barrier and Invade the Central Nervous System. Front. Microbiol. *10*, 525. https://doi.org/10.3389/fmicb.2019.00525.
46. Gavino-Leopoldino, D., Figueiredo, C.M., da Silva, M.O.L., Barcellos, L.G., Neris, R.L.S., Pinto, L.D.M., Araújo, S.M.B., Ladislau, L., Benjamim, C.F., Da Poian, A.T., et al. (2021). Skeletal Muscle Is an Early Site of Zika Virus Replication and Injury, Which Impairs Myogenesis. J. Virol. *95*, e0090421. https://doi.org/10.1128/JVI.00904-21.
47. Chan, J.F.W., Zhang, A.J., Chan, C.C.S., Yip, C.C.Y., Mak, W.W.N., Zhu, H., Poon, V.K.M., Tee, K.M., Zhu, Z., Cai, J.P., et al. (2016). Zika Virus Infection in Dexamethasone-immunosuppressed Mice Demonstrating Disseminated Infection with Multi-organ Involvement Including Orchitis Effectively Treated by Recombinant Type I Interferons. EBioMedicine *14*, 112–122. https://doi.org/10.1016/j.ebiom.2016.11.017.
48. Kurscheidt, F.A., Mesquita, C.S.S., Damke, G.M.Z.F., Damke, E., Carvalho, A.R.B.d.A., Suehiro, T.T., Teixeira, J.J.V., da Silva, V.R.S., Souza, R.P., and Consolaro, M.E.L. (2019). Persistence and clinical relevance of Zika virus in the male genital tract. Nat. Rev. Urol. *16*, 211–230. https://doi.org/10.1038/s41585-019-0149-7.
49. Caine, E.A., Scheaffer, S.M., Arora, N., Zaitsev, K., Artyomov, M.N., Coyne, C.B., Moley, K.H., and Diamond, M.S. (2019). Interferon lambda protects the female reproductive tract against Zika virus infection. Nat. Commun. *10*, 280. https://doi.org/10.1038/s41467-018-07993-2.
50. Zhang, Y., Sheng, Z., Gao, N., Wu, N., Wang, P., Fan, D., Zhou, D., Cheng, G., and An, J. (2022). Zika Virus Infection in the Ovary Induces a Continuously Elevated Progesterone Level and Compromises Conception in Interferon Alpha/Beta Receptor-Deficient Mice. J. Virol. *96*, e0118921. https://doi.org/10.1128/JVI.01189-21.
51. Barden, A., Phillips, M., Hill, L.M., Fletcher, E.M., Mas, E., Loh, P.S., French, M.A., Ho, K.M., Mori, T.A., and Corcoran, T.B. (2018). Antiemetic doses of dexamethasone and their effects on immune cell populations and plasma mediators of inflammation resolution in healthy volunteers. Prostaglandins Leukot. Essent. Fatty Acids *139*, 31–39. https://doi.org/10.1016/j.plefa.2018.11.004.
52. Brito, C.A.A., Henriques-Souza, A., Soares, C.R.P., Castanha, P.M.S., Machado, L.C., Pereira, M.R., Sobral, M.C.M., Lucena-Araujo, A.R., Wallau, G.L., and Franca, R.F.O. (2018). Persistent detection of Zika virus RNA from an infant with severe microcephaly – a case report. BMC Infect. Dis. *18*, 388. https://doi.org/10.1186/s12879-018-3313-4.
53. Ireland, D.D.C., Manangeeswaran, M., Lewkowicz, A.P., Engel, K., Clark, S.M., Laniyan, A., Sykes, J., Lee, H.-N., McWilliams, I.L., Kelley-Baker, L., et al. (2020). Long-term persistence of infectious Zika virus: Inflammation and behavioral sequela in mice. PLoS Pathog. *16*, e1008689. https://doi.org/10.1371/journal.ppat.1008689.
54. Michalski, D., Ontiveros, J.G., Russo, J., Charley, P.A., Anderson, J.R., Heck, A.M., Geiss, B.J., and Wilusz, J. (2019). Zika virus noncoding sfRNAs sequester multiple host-derived RNA-binding proteins and modulate mRNA decay and splicing during infection. J. Biol. Chem. *294*, 16282–16296. https://doi.org/10.1074/jbc.RA119.009129.
55. Chang, R.-Y., Hsu, T.-W., Chen, Y.-L., Liu, S.-F., Tsai, Y.-J., Lin, Y.-T., Chen, Y.-S., and Fan, Y.-H. (2013). Japanese encephalitis virus non-coding RNA inhibits activation of interferon by blocking nuclear translocation of interferon regulatory factor 3. Vet. Microbiol. *166*, 11–21. https://doi.org/10.1016/j.vetmic.2013.04.026.
56. Paolicelli, R.C., Sierra, A., Stevens, B., Tremblay, M.-E., Aguzzi, A., Ajami, B., Amit, I., Audinat, E., Bechmann, I., Bennett, M., et al. (2022). Microglia states and nomenclature: A field at its crossroads. Neuron *110*, 3458–3483. https://doi.org/10.1016/j.neuron.2022.10.020.
57. Manangeeswaran, M., Ireland, D.D.C., and Verthelyi, D. (2016). Zika (PRVABC59) Infection Is Associated with T cell Infiltration and Neurodegeneration in CNS of Immunocompetent Neonatal C57Bl/6 Mice. PLoS Pathog. *12*, e1006004. https://doi.org/10.1371/journal.ppat.1006004.
58. Zukor, K., Wang, H., Siddharthan, V., Julander, J.G., and Morrey, J.D. (2018). Zika virus-induced acute myelitis and motor deficits in adult interferon αβ/γ receptor knockout mice. J. Neurovirol. *24*, 273–290. https://doi.org/10.1007/s13365-017-0595-z.
59. Kung, P.-L., Chou, T.-W., Lindman, M., Chang, N.P., Estevez, I., Buckley, B.D., Atkins, C., and Daniels, B.P. (2022). Zika virus-induced TNF-α signaling dysregulates expression of neurologic genes associated with psychiatric disorders. J. Neuroinflammation *19*, 100. https://doi.org/10.1186/s12974-022-02460-8.
60. Almeida, R.d.N., Braz-de-Melo, H.A., Santos, I.d.O., Corrêa, R., Kobinger, G.P., and Magalhaes, K.G. (2020). The Cellular Impact of the ZIKA Virus on Male Reproductive Tract Immunology and Physiology. Cells *9*, 1006. https://doi.org/10.3390/cells9041006.
61. Matusali, G., Houzet, L., Satie, A.-P., Mahé, D., Aubry, F., Couderc, T., Frouard, J., Bourgeau, S., Bensalah, K., Lavoué, S., et al. (2018). Zika virus infects human testicular tissue and germ cells. J. Clin. Invest. *128*, 4697–4710. https://doi.org/10.1172/JCI121735.
62. Baud, D., Musso, D., Vouga, M., Alves, M.P., and Vulliemoz, N. (2017). Zika virus: A new threat to human reproduction. Am. J. Reprod. Immunol. *77*, e12614. https://doi.org/10.1111/aji.12614.
63. Huang, D., Wei, W., Xie, F., Zhu, X., Zheng, L., and Lv, Z. (2018). Steroidogenesis decline accompanied with reduced antioxidation and endoplasmic reticulum stress in mice testes during ageing. Andrologia *50*, e12816. https://doi.org/10.1111/and.12816.

64. Baba, T., Shima, Y., Owaki, A., Mimura, J., Oshima, M., Fujii-Kuriyama, Y., and Morohashi, K. -i. (2008). Disruption of Aryl Hydrocarbon Receptor (AhR) Induces Regression of the Seminal Vesicle in Aged Male Mice. Sex. Dev. *2*, 1–11. https://doi.org/10.1159/000117714.
65. Luo, L., Chen, H., and Zirkin, B.R. (2001). Leydig cell aging: steroidogenic acute regulatory protein (StAR) and cholesterol side-chain cleavage enzyme. J. Androl. *22*, 149–156. https://doi.org/10.1002/j.1939-4640.2001.tb02165.x.
66. Wang, Y., Chen, L., Xie, L., Li, L., Li, X., Li, H., Liu, J., Chen, X., Mao, B., Song, T., et al. (2018). Interleukin 6 inhibits the differentiation of rat stem Leydig cells. Mol. Cell. Endocrinol. *472*, 26–39. https://doi.org/10.1016/j.mce.2017.11.016.
67. Allen, J.A., Diemer, T., Janus, P., Hales, K.H., and Hales, D.B. (2004). Bacterial Endotoxin Lipopolysaccharide and Reactive Oxygen Species Inhibit Leydig Cell Steroidogenesis via Perturbation of Mitochondria. Endocrine *25*, 265–275. https://doi.org/10.1385/ENDO:25:3:265.
68. Parmar, A.R., Trivedi, P.P., and Jena, G.B. (2014). Dextran sulfate sodium-induced ulcerative colitis leads to testicular toxicity in mice: Role of inflammation, oxidative stress and DNA damage. Reprod. Toxicol. *49*, 171–184. https://doi.org/10.1016/j.reprotox.2014.08.004.
69. Avelino-Silva, V.I., Alvarenga, C., Abreu, C., Tozetto-Mendoza, T.R., Canto, C.L.M.d., Manuli, E.R., Mendes-Correa, M.C., Sabino, E.C., Figueiredo, W.M., Segurado, A.C., and Mayaud, P. (2018). Potential effect of Zika virus infection on human male fertility? Rev. Inst. Med. Trop. Sao Paulo *60*, e64. https://doi.org/10.1590/s1678-9946201860064.
70. Bujan, L., Mansuy, J.-M., Hamdi, S., Pasquier, C., and Joguet, G. (2020). 1 year after acute Zika virus infection in men. Lancet Infect. Dis. *20*, 25–26. https://doi.org/10.1016/S1473-3099(19)30678-4.
71. Coelho, S.V.A., Neris, R.L.S., Papa, M.P., Schnellrath, L.C., Meuren, L.M., Tschoeke, D.A., Leomil, L., Verçoza, B.R.F., Miranda, M., Thompson, F.L., et al. (2017). Development of standard methods for Zika virus propagation, titration, and purification. J. Virol. Methods *246*, 65–74. https://doi.org/10.1016/j.jviromet.2017.04.011.
72. Vogt, M.B., Frere, F., Hawks, S.A., Perez, C.E., Coutermarsh-Ott, S., and Duggal, N.K. (2021). Persistence of Zika virus RNA in the epididymis of the murine male reproductive tract. Virology *560*, 43–53. https://doi.org/10.1016/j.virol.2021.05.001.
73. Racine, R.J. (1972). Modification of seizure activity by electrical stimulation: II. Motor seizure. Electroencephalogr. Clin. Neurophysiol. *32*, 281–294. https://doi.org/10.1016/0013-4694(72)90177-0.

STAR★METHODS

KEY RESOURCES TABLE

REAGENT or RESOURCE	SOURCE	IDENTIFIER
Antibodies		
Rabbit Polyclonal anti-IBA-1	Wako Chemicals USA	Cat# 019–19741; RRID:AB_839504
Goat anti-rabbit Alexa 546	ThermoFisher Scientific	Cat# A-11035, RRID: AB_2534093
Bacterial and virus strains		
Zika virus, Gene bank: KX197192	Isolated from patient (Coelho, 2017)	N/A
Chemicals, peptides, and recombinant proteins		
Trizol®	Invitrogen™	Cat# 15596018
Fluoromount-G mounting medium	ThermoFisher Scientific	Cat# 00-4958-02
DAPI	ThermoFisher Scientific	Cat# D1306
Pentylenetetrazole	Sigma-Aldrich	Cat# P6500-25G
Dexamethasone	Fragon Ibérica	Cat# 30505-20
Cyclosporine	Sigma-Aldrich	Cat# 59865-13-3
Critical commercial assays		
High-Capacity cDNA Reverse Transcription Kit	Applied Biosystems™	Cat# 4368814
Power SYBR Green Master Mix	Applied Biosystems™	Cat# 4368702
TaqMan Mix kit	Applied Biosystems™	Cat# 4369016
Ambion™ DNase I (RNase-free)	Invitrogen™	Cat# AM2222
DeadEnd™ Fluorometric TUNEL System	Promega Corporation	Cat# G3250
Rapid Panoptic Kit	Laborclin	Cat# 620529
Experimental models: Organisms/strains		
Swiss mice male and female 3 months old	Charles River Laboratories and bred in our facility	N/A
Oligonucleotides		
IFN-β: Forward: 5′ CCA CTT GAA GAG CTA TTA CTG 3′; Reverse: 5′ AAT GAT GAG AAA GTT CCT GAA G 3′	ThermoFischer Scientific	N/A
ISG15: Forward: 5′AAC TGC AGC GAG CCT CTG A 3′; Reverse: 5′CAC CTT CTT CTT AAG CGT GTC TAC AG 3′	ThermoFischer Scientific	N/A
OAS1: Forward: 5′ TCC ACA GTA CGC CCT AGA GT 3′; Reverse: 5′ GAC CAG TTC CAA GAC GGT CC 3′	ThermoFischer Scientific	N/A
TNF-α: Forward: 5′-CCT CAC ACT CAG ATC ATC TTC TCA-3′; Reverse: 5′-TGG TTG TCT TTG AGA TCC ATG C-3′	ThermoFischer Scientific	N/A
IL1-β: Forward: 5′- GTA ATG AAA GAC GGC ACA CC-3′; Reverse: 5′- ATT AGA AAC AGT CCA GCC CA - 3′	ThermoFischer Scientific	N/A
IL6: Forward: 5′- TCA TAT CTTCAA CCA AGA GGTA-3′; Reverse: 5′-CAG TGA GGA ATG TCC ACA AAC TG-3′	ThermoFischer Scientific	N/A
3β-HSD: Forward: 5′-CGG CTG CTG CAC AGG AAT AA-3′; Reverse: 5′-GAT GCT GAT CTC CTC AGC CC-3′	ThermoFischer Scientific	N/A
CYP11A1: Forward: 5′- GAC CTG GAA GGA CCA TGC A -3′; Reverse: 5′- TGG GTG TAC TCA TCA GCT TTA TTG A -3′	ThermoFischer Scientific	N/A
StAR: Forward: 5′- CAG TCC CGG GTG GAT GGG TCA-3′; Reverse: 5′- TCC CCG TTC TCC TGC TGG CT-3′	ThermoFischer Scientific	N/A
XRN1: Forward: 5′-TTA TGG CTG TTG ACG GTG TG-3′; Reverse: 5′-TGG CTG ACC TAA AAC GCC TC-3′	ThermoFischer Scientific	N/A

(*Continued on next page*)

Continued

REAGENT or RESOURCE	SOURCE	IDENTIFIER
Actin: Forward: 5′-TGT GAC GTT GAC ATC CGT AAA-3′; Reverse: 5′-GTA CTT GCG CTC AGG AGG AG-3′	ThermoFischer Scientific	N/A
ZIKV RNA: Forward: 5′-CCG CTG CCC AAC ACA AG-3′; Reverse: 5′-CCA CTA ACG TTC TTT TGC AGA CAT-3′	ThermoFischer Scientific	N/A
E protein sequence: 5′-rCrGrG rArCrA rGrCrC rGrCrU rGrCrC rCrArA rCrArC rArArG rGrUrG rArArG rCrCrU rArCrC rUrUrG rArCrA rArGrC rArArU rCrArG rArCrA rCrUrC rArArU rArUrG rUrCrU rGrCrA rArArA rGrArA rCrGrU rUrArG rUrGrG rArCrA rGrArG-3′	ThermoFischer Scientific	N/A
Subgenomic Flavivirus RNA: Forward: 5′-CTG CTA GTC AGC CAC AGC TT-3′; Reverse: 5′-CTG ATC TCC AGT TCA GGC CC-3′	ThermoFischer Scientific	N/A
NS5 gene: Forward: 5′- CCT TGG ATT CTT GAA CGA GGA -3′; Reverse: 5′- AGA GCT TCA TTC TCC AGA TCA A-3′	ThermoFischer Scientific	N/A
Software and algorithms		
ImageJ v1.53	NIH	https://imagej.net/ij/
GraphPad Prism 8	Graphpad	https://www.graphpad.com/
ANY-maze	ANY-maze	https://www.any-maze.com/

RESOURCE AVAILABILITY

Lead contact

Any additional information and requests for resources and reagents should be directed to and will be fulfilled by lead contact, Julia R. Clarke (juclarke@gmail.com; julia.clarke@icb.ufrj.br).

Materials availability

This study did not generate new unique reagents.

Data and code availability

Data reported in this paper will be shared by the lead contact upon request. This paper does not report original code. Any additional information required to reanalyze the data reported in this paper is available from the lead contact upon request.

EXPERIMENTAL MODEL AND STUDY PARTICIPANT DETAILS

Experimental design

Adult Swiss mice were mated, and pregnant females were housed in individual cases. Pups at postnatal day 3 (P3) were infected with 10^6 PFU of ZIKV. When they reached adulthood (P60) they were submitted to daily pharmacological treatment with either dexamethasone (DX) or cyclosporine (Cyclo) for up to ten days. Behavioral assessment and tissue collection were performed before (time 0), or after 2, 5 or 10 days of treatment as indicated.

Animals

Male and female Swiss mice were mated for two weeks in a harem system (4 females per male) at room temperature between 20°C and 22°C, 12h light-dark cycle. Two weeks after mating, pregnant dams were placed in individual boxes until the offspring were born. Litters were normalized to 8–10 animals per offspring, where the number of male and female pups was kept equal whenever possible. All pups from each litter received the same treatment to avoid cross-contamination. Animals were weaned at postnatal day 21 and housed with 2–5 same-sex littermates. During the whole experiment, animals had free access to filtered water and certified chow. Litters were evaluated daily for mortality and signs of illness. All procedures performed in the present study were approved by the Institutional Committee for Animal Care and Use of the Federal University of Rio de Janeiro (protocol nº 093/19) and followed the ARRIVE guidelines.

METHOD DETAILS

Virus

Zika virus was isolated from a febrile case in the state of Pernambuco, Brazil (gene bank KX197192).[71] C6/36 cells were infected at a multiplicity of infection (MOI) of 0.01, in non-supplemented L15 culture medium (Leibovitz's medium) at 28°C for 1 h. After this period, the medium was removed and the cells maintained in L15 medium supplemented with 5% fetal bovine serum (FBS) at 28°C for 7 days. The culture supernatant was clarified by centrifugation at 5,000 rpm for 10 min, then aliquoted and stored at −80°C. Plaque lysis assays were performed on VERO cells to determine the titer of viral stocks. These cells were grown on 24-well plates at 37°C and 5% CO_2, and were infected with 200 μL of the serial dilutions (10^{-1} to 10^{-6}) of the virus in Dulbecco's Modified Eagle's Medium (DMEM – Sigma-Aldrich, Saint Louis, MO) high glucose, and incubated for 1 h in the same culture environment. Then, 1 mL of DMEM high glucose medium with 1.5% carboxymethylcellulose (CMC – Sigma-Aldrich, Saint Louis, MO), 1% FBS and 1% penicillin/streptomycin (ThermoFisher Scientific Inc, *Waltham, MA*) was added to each well. After 5 days, cells were fixed with 10% formaldehyde (Sigma-Aldrich, Saint Louis, MO) and stained with dye solution (20% Ethanol, 1% Crystal Violet and H_2O_2) for 30 min, thus allowing visualization and counting of the plaque-forming units (UFP).

Viral infections

On the third day after birth (postnatal day 3, P3) male and female mice received a subcutaneous (s.c., in the dorsum of pups) injection of 30 μL containing 10^6 PFU of ZIKV, whereas control groups received the same volume of mock (conditioned medium of C6/36 cells cultured without the virus). Litters were assessed daily for mortality.

Pharmacological treatments

Dexamethasone (DX)

Treatment began at 60 days post-infection (dpi). Chan et al. (2016)[47] found that adult immunocompetent mice treated with this dose of DX for ten days became susceptible to peripheral ZIKV infection. Therefore, in our study animals received daily injections of 50 mg/kg body weight of dexamethasone (Fragon Ibérica, Barcelona, Espanha, Cat# 30505-20) intraperitoneally (i.p)[47] for 2, 5 or 10 consecutive days. Control groups received an equal volume of 0.9% sterile saline solution. Body weight was monitored throughout treatment.

Cyclosporine (Cyclo)

Treatment began at 60 dpi. Animals received daily injections of 30 mg/kg body weight of cyclosporine (Sigma-Aldrich, Saint Louis, MO, Cat# 59865-13-3i.p.) for 10 consecutive days. Dose and time of treatment were chosen based on previous studies.[72] Control groups received an equal volume of 0.9% sterile saline solution.

Tissue collection and preparation

At different timepoints of DX or Cyclo treatment, mice were deeply anesthetized (80 mg/kg ketamine and 10 mg/kg xylazine, i.p.) and samples of brain, epididymis, spleen, testicles, ovaries and gastrocnemius muscle were collected. Testicles were collected in an Eppendorf tube and weighed on an analytical weighing scale (Marte Científica e Instrumentação LTDA, Belo Horizonte, Brazil). The samples were then frozen in liquid nitrogen and stored at −80°C until RNA extraction began.

Behavioral tests

Open field

For measurement of locomotor and anxiety-like behavior, mice were placed in the center of the open field apparatus (measuring 30 × 30 × 45 cm) and allowed to freely explore the arena for 5 min. The experiment was carried out with an indirect light source and the whole session was filmed. Using the ANY-maze software (Stoelting Company, Wood Dale, IL), the total distance traveled and the amount of time spent by each mouse in the center of the box were quantified. The arena was thoroughly cleaned with 70% ethanol in between trials to eliminate olfactory cues.

Pentylenetetrazole (PTZ)

Adult male mice received an i.p. injection of the GABA antagonist pentylenetetrazol (50 mg/kg; Sigma-Aldrich, Saint Louis, MO, Cat# P6500-25G). Subsequently, the animals were placed in empty 3 L glass beakers and their behavior was analyzed by a trained researcher blind to experimental conditions, during 15 min. The time elapsed until the animals presented the first seizure episode as well as the number of seizures during the session were analyzed, according to the Racine scale.[73] The beakers were cleaned with 70% ethanol in between trials to eliminate olfactory cues. Animals that had no seizure episodes during the entire observation period, were excluded from further analysis.

RNA extraction and qPCR

Tissue RNA extraction was performed using TRIzol (Invitrogen, *Waltham, MA*, Cat# 15596018) using the piston for tissue homogenization according to manufacturer's instructions. RNA concentration and purity were determined by absorbance ratios of 260/280 and 260/230 nm measured in a NanoDrop 1000 spectrophotometer (ThermoFisher Scientific Inc, *Waltham, MA*). Only samples with absorbance ratios >1.8

were used. One microgram of total RNA was used for cDNA synthesis using the High-Capacity cDNA Reverse Transcription Kit (Applied Biosystems, *Waltham, MA,* Cat# 4368814). To quantify the mRNA of inflammatory genes and genes from the steroidogenic pathway, 10 ng of template cDNA were analyzed in a QuantStudio 5 PCR System (Applied Biosystems, Foster City, CA) with reactions performed in triplicate using the Sybr Green Master Mix kit (Applied Biosystems, *Waltham, MA,* Cat# 4368702), with all steps in accordance with the manufacturer's instructions. Primer sequences are shown on Table S1. Cycle threshold (Ct) values were normalized to a housekeeping gene (Actin) and analyzed using the ΔΔCt method to generate fold change values relative to control groups.

For viral quantification, real-time PCR analyses were performed on an Applied Biosystems 7500 RT-PCR system using the TaqMan Mix kit (Applied Biosystems, *Waltham, MA,* Cat# 4369016). Primers used for ZIKV RNA amplification were: forward: 5′-CCG CTG CCC AAC ACA AG-3′; reverse: 5′-CCA CTA ACG TTC TTT TGC AGA CAT-3′; Reporter: 5 ′-/56-FAM/AGC CTA CCT/ZEN/TGA CAA GCA ATC AGA CAC TCA A/3IABkFQ/-3′ (Integrated DNA Technologies), which amplify a region of E protein, as described by.[13] The ZIKV RNA copy number was determined using an amplification standard curve from 109 to 101 copies of a synthetized and reversed transcribed ZIKV RNA oligonucleotide corresponding to the amplified fragment (ZIKV synthetic RNA sequence: 5′-rCrGrG rArCrA rGrCrC rGrCrU rGrCrC rCrArA rCrArC rArArG rGrUrG rArArG rCrCrU rArCrC rUrUrG rArCrA rArGrC rArArU rCrArG rArCrA rCrUrC rArArU rArUrG rUrCrU rGrCrA rArArA rGrArA rCrGrU rUrArG rUrGrG rArCrA rGrArG-3′). Lower limits of detection were determined as CT values of 36 or higher for spleen, brain, epididymis and skeletal muscle whereas values of 35 or higher were considered negative for ZIKV in samples of testicles and ovaries.

Relative subgenomic flaviviral RNA (sfRNA) detection

RNA was extracted from brain samples as described above and sfRNA accumulation relative to the amount of genomic RNA was evaluated by RT-PCR. A single fragment in the 3′SL region in the 3′UTR of ZIKV genome was amplified using primers: forward, 5′-CTG CTA GTC AGC CAC AGC TT-3′, and sfRNA reverse, 5′-CTG ATC TCC AGT TCA GGC CC-3′. These primers targeted the nucleotides **10.404** to **10.639**, including primer sequences, from the ZIKV genome. ΔCt values were calculated by normalizing sfRNA Ct with amplification of the 3′ RNA extremity, corresponding to the NS5 gene (nucleotides **9.134** to **9.325**, also including primer sequences). Primer sequences used for amplification at the NS5 region were Fwd, 5′- CCT TGG ATT CTT GAA CGA GGA -3′; Rev, 5′- AGA GCT TCA TTC TCC AGA TCA A-3′, and data were expressed as $2^{-\Delta Ct}$.

Differential leukocyte count

A drop of blood was obtained from a small tail incision. Blood smear was used for differential leukocyte count before dexamethasone treatment (Day 0) and at 5 and 10 days of treatment with dexamethasone or saline. Rapid Panoptic Kit (Laborclin, Curitiba, Brazil, Cat# 620529) was used for hematological staining, with all steps in accordance with the manufacturer's instructions, and 100 leukocytes per slide were classified using an optical microscope Eclipse 50i light microscopy (Nikon, Tokyo, Japan). Morphological aspects of the cells were used to classify them as neutrophils, lymphocytes, macrophages, basophils or eosinophils. The percentage of lymphocytes was determined.

Tissue preparation and morphological analysis

Mice were deeply anesthetized with ketamine (80 mg/kg) and xylazine (10 mg/kg) before transcardial perfusion with 50 mL of Phosphate Buffered Saline (PBS, 0.1 M, pH 7.4) per animal followed by ice-cold 4% paraformaldehyde (PFA). Testicle and brain samples were dissected and post-fixed for 24 h in PFA 4%.

After fixation, testicles tissues were included in paraffin blocks and 5 μm-thick sections were obtained in a Leica microtome (Leica, Wetzlar, Germany). Tissue sections were stained with hematoxylin and eosin (H&E) and subsequently photographed by Eclipse 50i light microscopy (Nikon, Tokyo, Japan).

Fifty μm coronal sections were obtained from post-fixed brains using a VT1000S vibratome (Leica, Wetzlar, Germany), and stored in PBS at 2°C. Immunohistochemistry was performed with free floating sections. After standard antigenic retrieval, sections were permeabilized with 0.1% Triton X-100 (Sigma-Aldrich, Saint Louis, MO), blocked with 3% goat serum albumin Sigma-Aldrich, Saint Louis, MO) in PBS for 2h, and incubated with anti-Iba-1 (1:1000; FUJIFILM Wako Chemicals, Richmond, VA; Cat# 019–19741, RRID: AB_839504) overnight. Then, sections were washed with PBS and incubated with secondary antibody goat anti-rabbit Alexa 546 (1:500; ThermoFisher Scientific Inc, *Waltham, MA* Cat# A-11035, RRID: AB_2534093). Nuclei were stained with DAPI (0.5 mg/mL, ThermoFisher Scientific Inc, *Waltham, MA*, Cat# D1306) for 20 min and slides were then mounted with fluoromount-G mounting medium (ThermoFisher Scientific Inc, *Waltham, MA*, Cat# 00-4958-02). Images from the supragranular layer of the somatosensory cortex were acquired with a TCS SP8 confocal microscope (Leica, Wetzlar, Germany) with a 63x objective. Sholl analyses were performed in 4–6 cells per section, using Fiji software as describe below. Z-stacks were used for determination of the maximum intensity projection of Iba-1 positive channel, to allow visualization of all microglia processes. The despeckle filter was used to reduce background noise. Then, a binary mask was created by thresholding the images. Iba-1 positive cells were manually selected, and the Sholl analysis was done using Fiji (ImageJ, National Institute of Health, USA) neuroanatomy plugin.

TUNEL assay

Quantitation of apoptotic cells were performed by TUNEL assay method using the DeadEnd Fluorometric TUNEL System following manufacturer's instructions (Promega Corporation, Madison, WI). Images were obtained on a Sight-DS-5M-L1 digital camera (Nikon, Melville, NY, Cat# G3250) connected to an Eclipse 50i light microscope (Nikon, Melville, NY). The total number of TUNEL-positive cells per section were

counted by a researcher blind to experimental conditions. At least two sections from each animal were analyzed, averaged, and plotted on the bar graph.

QUANTIFICATION AND STATISTICAL ANALYSIS

Statistical analysis

Graphs and statistical analysis were performed using GraphPad Prism 8 (GraphPad Software, Boston, MA). Data are expressed as means ± SEM and the identification of outliers was evaluated using the ROUT test. D'Agostino-Pearson normality test used to assess the Gaussian distribution of the data. Student's *t* tests were performed to compare two groups with comparable variances and the *t* test with Welch's correction was applied when comparing two groups with unequal variances. One-way ANOVA with post-hoc tests was performed to compare 3 or more groups. Lymphocyte counts across treatment were analyzed by two-Way ANOVA, and body weight was analyzed by repeated measures two-Way ANOVA. Mann-Whitney test was performed to compare groups with nonparametric distribution. *p* values were calculated for each experiment and *p* values smaller than 0.05 were considered statistically significant. Information on statistical tests applied and *p* values obtained are described in the corresponding figure legend.